"Job-Sharing" Storage of Hydrogen in Ru/Li 2 O Nanocomposites

ARTICLE *in* NANO LETTERS · APRIL 2015

Impact Factor: 13.59 · DOI: 10.1021/acs.nanolett.5b01320 · Source: PubMed

NANO LETTERS

Letter

pubs.acs.org/NanoLett

"Job-Sharing" Storage of Hydrogen in Ru/Li_2O Nanocomposites

Lijun Fu,*[,†] Kun Tang,[†] Hyunchul Oh,[‡,∥] Kandavel Manickam,[‡] Thomas Bräuniger,[†] C. Vinod Chandran,[†] Alexander Menzel,[§] Michael Hirscher,[‡] Dominik Samuelis,*[,†] and Joachim Maier*[,†]

[†]Max Planck Institute for Solid State Research, Heisenbergstrasse 1, Stuttgart, Germany

[‡]Max Planck Institute for Intelligent Systems, Heisenbergstrasse 3, Stuttgart, Germany

[§]Institute of Physical Chemistry, University of Innsbruck, Innrain 80-82, Innsbruck, Austria

[∥]Korea Institute of S&T Evaluation and Planning, 137-739, Trust Tower 60 Mabang-ro, Seocho-gu Seoul, Korea

Supporting Information

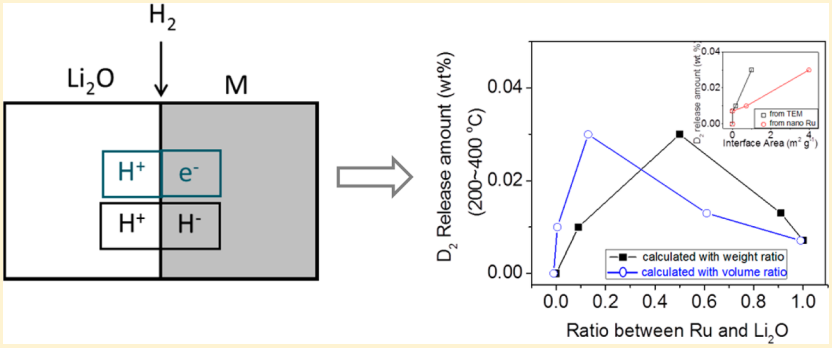

ABSTRACT: A "job-sharing" hydrogen storage mechanism is proposed and experimentally investigated in Ru/Li_2O nanocomposites in which H^+ is accommodated on the Li_2O side, while H^- or e^- is stored on the side of Ru. Thermal desorption-mass spectroscopy results show that after loading with D_2, Ru/Li_2O exhibits an extra desorption peak, which is in contrast to Ru nanoparticles or ball-milled Li_2O alone, indicating a synergistic hydrogen storage effect due to the presence of both phases. By varying the ratio of the two phases, it is shown that the effect increases monotonically with the area of the heterojunctions, indicating interface related hydrogen storage. X-ray diffraction, Fourier transform infrared spectroscopy, and nuclear magnetic resonance results show that a weak LiO···D bond is formed after loading in Ru/Li_2O nanocomposites with D_2. The storage–pressure curve seems to favor H^+/H^- over H^+/e^- mechanism.

KEYWORDS: *Hydrogen storage mechanism, interfacial storage, ruthenium, Li_2O*

In the context of electrochemical energy conversion, that is, of fuel cells and batteries, the storage of light elements, such as hydrogen and lithium, plays a major role and will become increasingly important for future energy supply chains. Being able to quickly and efficiently store hydrogen in great amounts at low overall weight would not only be a decisive step forward in the application of fuel cells but also a great step toward the utilization of sustainable intermittent energy sources such as light and wind.[1]

Of more fundamental interest is it to identify possible storage mechanisms other than the storage in pure form in pressurized tanks or as cryogenic liquid hydrogen. The simplest known mechanism is to store hydrogen at the surfaces of appropriate materials by adsorption. This storage mode does not involve strong bonding and allows for a rapid release. Typical materials include nanostructured carbon materials.[2,3] Metal–organic framework composites (MOFs)[4] can be subsumed under this mechanism, too, because of their ability to accommodate hydrogen owing to the large internal space and the weak bonding. More precisely this mechanism belongs to, or at least forms the bridge to the second mechanism in which hydrogen is absorbed in the form of bulk storage. During such a dissolution, the underlying structure stays basically constant and only the defect chemistry varies. Examples can be found in the first stage of hydrogen storage in metals, such as Mg[5] and FeTi.[6] A third mechanism relies on phase transformation induced when the solubility limit is exceeded, and a new H-rich phase is formed with the pressure isotherm showing a flat plateau. The dissolution and phase transformation reactions can be distinguished according to the composition trajectory in the phase diagram. The fourth mechanism refers to a reduction of a phase down to a palette of products, that is, to a conversion reaction. One example is Li_3N, which is believed to react according to $Li_3N + 2H_2 \leftrightarrow Li_2NH + LiH + H_2 \leftrightarrow LiNH_2 + 2LiH$.[7,8] It is sensible to count this mechanism separately, as the microstructural complexity hinders reversibility substantially.

In this work, we demonstrate the occurrence of a fifth hydrogen storage mechanism, based on synergistic storage at

Received: April 5, 2015
Published: April 27, 2015

DOI: 10.1021/acs.nanolett.5b01320
Nano Lett. 2015, 15, 4170–4175

two-phase contacts. Such a "job-sharing" mechanism has been recently discussed and characterized for Li storage.[9] Nanocomposites of Ru/Li_2O or Ni/LiF have been shown to be able to store Li, even though neither of the constituent phases is able to do so alone: Li_2O has plenty of room to interstitially store Li^+, yet cannot accommodate the e^-; Ru as a noble metal can easily store the e^- but not Li^+. In contrast to the individual phases, the composites can store Li.[9−11] This can be generalized to the storage of a component A^+B^- that may be stored by a composite α/β, where α can store A^+ but not B^-, while the opposite is given for β. Should this be an option for the storage of hydrogen, one phase must be basic enough to store H^+, while the other phase must act as e^- or H^- acceptor. We chose Ru/Li_2O nanocomposites here as a model system, which has been investigated extensively in battery research due to its unique electrochemical properties.[9,10,12−15] Assuming $H_2 + (\alpha/\beta) = 2\ H^+(\alpha) + 2\ e^-(\beta)$, exactly a composite of Li_2O and Ru should be a suitable candidate. Here a job-sharing mechanism according to $H_2 + (\alpha/\beta) = H^+(\alpha) + H^-(\beta)$ is possible as well. Surface hydrogen on Ru has been investigated in ref 16; under high pressure, Ru even shows hydrogen solubility.[17] Beside its basic properties, Li_2O has been chosen to be one component of the composite for investigation of the "job-sharing" mechanism because it allows us to exclude a competing mechanism based on hydrogen storage by spillover. In this mechanism, hydrogen is dissociated on the surface of a transition metal component and the atomic hydrogen then transfers to the surface of a second component. This process would not happen for the second component alone under the same conditions.[18] The spillover effect is not expected to happen for Ru/Li_2O, as it is energetically unfavorable to have H atoms spillover to a nonreducible support, such as Li_2O. Accommodation of electrons even in the form of F centers (anionic vacancies in a crystal filled by electrons) has been shown to be very unfavorable for Li_2O.[19,20] To avoid misunderstandings, in this contribution we demonstrate a novel way of storage that completes the palette of possible mechanisms rather than suggesting a technologically relevant synergistic storage mode. The two publications that come closest to our report refer to hydrogenation catalysis in $Au-CeO_2$[21] and Ru−MgO[22] composites where a dissocation of dihydrogen to form metal hydride and hydrogen groups on the oxide has been assumed. In these examples, the possibilities of homogeneous reduction effects ($Au-CeO_2$) and the lack of direct evidence (Ru−MgO) do not allow one to draw unambiguous conclusions on a space charge mechanism. Moreover, a dependence on the contact area has not been given.

Let us start with a thermodynamic analysis of the "job-sharing" hydrogen storage at the interface of α and β phases. When H^+/e^- heterogeneous storage reaction

$$\frac{1}{2}H_2 \rightleftharpoons H^+(\alpha) + e^-(\beta) \tag{1}$$

is considered, the heterogeneous mass action law can be formulated[23,9]

$$P_{H_2}^{1/2} = K^{\alpha/\beta} i_0(\alpha) n_0(\beta) \tag{2}$$

where $n \equiv$ concentration of conduction electrons, $i \equiv$ concentration of H^+-interstitials, $P \equiv$ partial pressure; the subscript 0 denotes the adjacent lattice planes directly at the interface. As the first case, we consider the contact of two nonmetallic materials. It can be stated that for the charges ($|Q_{H^+}{}^{\alpha}| \propto \int i^{\alpha} dx$); ($|Q_{e^-}{}^{\beta}| \propto \int n^{\beta}\, dx$), where $Q_{H^+}{}^{\alpha} = -Q_{e^-}{}^{\beta}$. As two Gouy−Chapman profiles are obtained from the Poisson−Boltzmann equation, it holds that

$$|Q_{H^+}{}^{\alpha}| \propto \sqrt{\varepsilon^{\alpha} i_0^{\alpha}} \simeq \sqrt{\varepsilon^{\beta} i_0^{\beta}} \propto |Q_{e^-}{}^{\beta}| \tag{3}$$

where $Q_H \equiv Q_{H^+} \equiv -Q_{e^-}$, owing to global electroneutrality, ($i_0^{\alpha} \simeq (\varepsilon^{\beta}/\varepsilon^{\alpha}) n_0^{\beta}$). If we combine eq 2 with eq 3, we find $P_{H_2} \propto Q_H^8$. As the second case, we refer to the situation that the β phase is a metal. Here the charge density is concentrated on the first layer, thus $Q_{e^-}{}^{\beta} = n_0{}^{\beta}$. Then one derives $P_{H_2} \propto Q_H^6$.

When the heterogeneous hydrogen storage reaction

$$H_2 \rightleftharpoons H^+(\alpha) + H^-(\beta) \tag{4}$$

is considered, analogously one derives $P_{H_2} \propto Q_H^4$ for two nonmetallic phases and $P_{H_2} \propto Q_H^3$ for the situation that the β phase is metal.

In the above treatment, we have neglected the electrical potential drop between outmost layer of two contacted phases, which is permissible here (in contrast to Li storage[9]), becauseof Q being small. For a more general treatment, see ref 9. The exponents in the relation of $P_{H_2} \propto Q_H^n$ in different mechanisms are listed in Table 1.

Table 1. Dependence of the Hydrogen Storage Capacity Q_H on Hydrogen Pressure P_{H_2} in Thermodynamic Equilibrium (where IC Denotes Ionic Conductor, SC Is Semiconductor, and M Is Metal) for Low Storage

	value of n in $P_{H_2} \propto Q_H^n$	
contacted phases	H^+/e^- mechanism	H^+/H^- mechanism
IC/SC	8	4
IC/M	6	3

Ru/Li_2O composites were prepared via electrochemically lithiation of RuO_2, or ball-milling of Ru and Li_2O with dimethyl carbonate (DMC) or *n*-hexane (details see Supporting Information). TEM images of Ru/Li_2O prepared by ball-milling method with DMC as milling solvent and heat-treated lithiated samples are shown in Supporting Information Figure S1. The nanocomposites present different parts with gray and black colors in the TEM image, which can be assigned as Li_2O and ruthenium by energy dispersive X-ray spectroscopy (EDX) measurement. The soft Li_2O is found to coat part of the surface of ruthenium particles or particle aggregates.

The high-pressure hydrogen storage capacity of Ru/Li_2O (1:1 wt %) was examined by sorption/desorption isotherm up to 20 bar at RT. The maximum hydrogen uptake at 20 bar for sample ball milled with DMC (1:1 wt %) is ca. 0.25 wt % (Supporting Information Figure S2). The hysteresis of the desorption process might be due to the ruthenium hydride formation at high pressure.[17] In the following study, we select the hydrogen loading pressure as 500 mbar to avoid possible high-pressure ruthenium hydride formation and to investigate the validity of the proposed interfacial storage mechanism, especially occurring between 0 and 1 bar.

Thermal desorption-mass spectroscopy (TDS-MS)[24] is used to investigate the hydrogen storage properties of Ru/Li_2O nanocomposites. The hydrogen storage performance of pure ruthenium nanoparticles (produced by reduction of RuO_2), of

DOI: 10.1021/acs.nanolett.5b01320
Nano Lett. 2015, 15, 4170−4175

Li_2O (ball-milled in DMC) and of Ru/Li_2O (ball-milled in DMC) is shown in Figure. 1. For Li_2O, there is no D_2

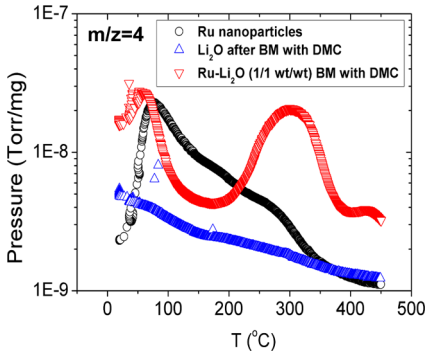

Figure 1. TDS-MS spectra of ruthenium nanoparticles, Li_2O and Ru–Li_2O nanocomposites (ball-milled with DMC) (heating rate: 0.1 °C/s).

desorption trace obtained during TDS measurement. As to the ruthenium nanoparticles, the desorption of D_2 takes place at low temperature, facilitated by rather mobile D species bound on ruthenium.[25,26] In contrast, for Ru/Li_2O, besides a similar D_2 desorption peak ranging in the temperature range of 20–100 °C, resulting from the deuterium adsorption on ruthenium, another desorption peak is observed from 200 to 400 °C. The new desorption peak only shows up for Ru/Li_2O but for neither of the two components, demonstrating the synergistic storage mechanism presents in Ru/Li_2O. Such a high desorption temperature indicates that the deuterium atom is rather chemically bound in the nanocomposites, which is proved by the solid-state NMR measurements (discussed later). TDS-MS spectra of Ru/Li_2O prepared via different methods are summarized in Supporting Information Figure S3. All samples show similar desorption behavior, indicating that the hydrogen storage performance is independent of preparation methods and impurities left or introduced. Note that there are no major water (HDO, D_2O) traces detected during the TDS measurements (Supporting Information Figure S4), ruling out formation and subsequent decomposition of LiOD species along 2LiOD + heat → Li_2O + D_2O as a majority storage mechanism.

Ru/Li_2O with different weight ratios prepared by ball-milling in DMC solvent show similar D_2 desorption behavior but with different release in the temperature range of 200 to 400 °C (Supporting Information Figure S5). As mentioned above, we ascribe the D_2 desorption in the higher temperature range to the contact of Ru nanoparticles and Li_2O in the composites. Figure 2 summarizes for Ru/Li_2O the calibrated amounts of desorbed D_2 for this temperature range and for various weight ratios. Ru/Li_2O of weight ratios of 1, 0.91, 0.50, 0.09, and 0 (with volume ratio of 1, 0.62, 0.14, 0.02, and 0) deliver 0.007, 0.013, 0.03, 0.01, and 0 wt % D_2 in the temperature range of 200 to 400 °C, respectively. Varying weight/volume ratio of nanocomposites corresponds to a variation of the interface area between two components in the nanocomposites. The resulting monotonic increase of the D_2 desorption amount (inset in Figure 2) with increasing contact area strongly supports the presence of a synergistic hydrogen storage mechanism. The agglomeration of ductile ruthenium during the ball-milling process could be the reason that Ru/Li_2O with a volume ratio of 0.14 shows higher hydrogen uptake than for a volume ratio

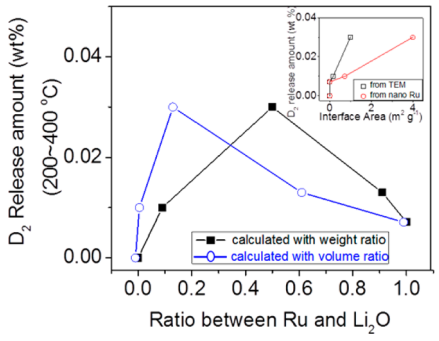

Figure 2. D_2 desorption amount of Ru, Li_2O, and Ru–Li_2O (ball-milled with DMC) with different ratios (in the temperature range of 200–400 °C). The inset shows the relation between D_2 desorption amount and the interface area of Li_2O and Ru phases. The method to estimate the interface area is described in the Supporting Information.

of 0.62. The uptake/desorption process in Ru/Li_2O cannot be cycled for the TDS measurement, which might be due to the change of nanocomposites microstructure during the heat-treatment, while the hydrogen uptake/desorption behavior is reversible for the isothermal experiment with long time evacuation (approximately 2 days) to release the uptaken hydrogen (see Supporting Information Figure S2).

The hydrogen storage mechanism was investigated using different methods. XRD results indicate that there is no phase change before and after D_2 uptake for Ru/Li_2O (ball-milled with DMC, 1:1 wt %, the sample is used for further analysis, if not mentioned specifically.). For ruthenium, no cell volume or lattice parameter changes were observed either (Supporting Information Figure S6).

FTIR spectroscopy was applied to Ru/Li_2O composites (ball-milled, DMC as solvent) before and after D_2 uptake and after TDS measurements. For the sample ball-milled with DMC (Figure 3a), typical absorption peaks of Li_2O[27] and impurities[28] introduced during preparation can be observed (details in Supporting Information 3). A new absorption peak appears at 2708 cm^{-1} after D_2 uptake and disappears after TDS measurement (Figure 3b), indicating the presence of an O···D bond in a LiO···D phase that was formed after loading D_2[29] and decomposed after D_2 desorption. The new absorption peak cannot be ascribed to the stretching mode of –OD in D_2O, which appears at ~2500 cm^{-1}.[30,31] Ball-milled Ru/Li_2O with hexane as the solvent (1:1 wt %) was investigated by FTIR spectroscopy. As shown in Figure 3c, no impurities are observed but only the typical infrared spectra of Li_2O. Similar as the ball-milled sample prepared in DMC, a new peak is present at 2708 cm^{-1} after D_2 loading but vanishes after TDS measurement (Figure 3d).

Solid-state NMR line-shape analysis is a powerful and sensitive technique for the characterization of the binding environments of elements.[32] ^2H static and ^7Li MAS NMR spectra were recorded for the D_2-loaded samples. The ^7Li MAS NMR spectra in Supporting Information Figure S7 show practically no difference of line shape between deuterium loaded Li_2O and Ru/Li_2O. The 2.80 ppm chemical shift corresponds to that observed for Li_2O.[14] If dipolar coupling of deuterium to lithium occurs at all then it would be very small, so no effect of ^2H on the ^7Li MAS NMR spectrum is actually expected. In contrast, the static ^2H NMR spectra show a drastic difference for the two host materials. As can be seen from Figure 4, only a narrow line is observed in the ^2H NMR

DOI: 10.1021/acs.nanolett.5b01320
Nano Lett. 2015, 15, 4170–4175

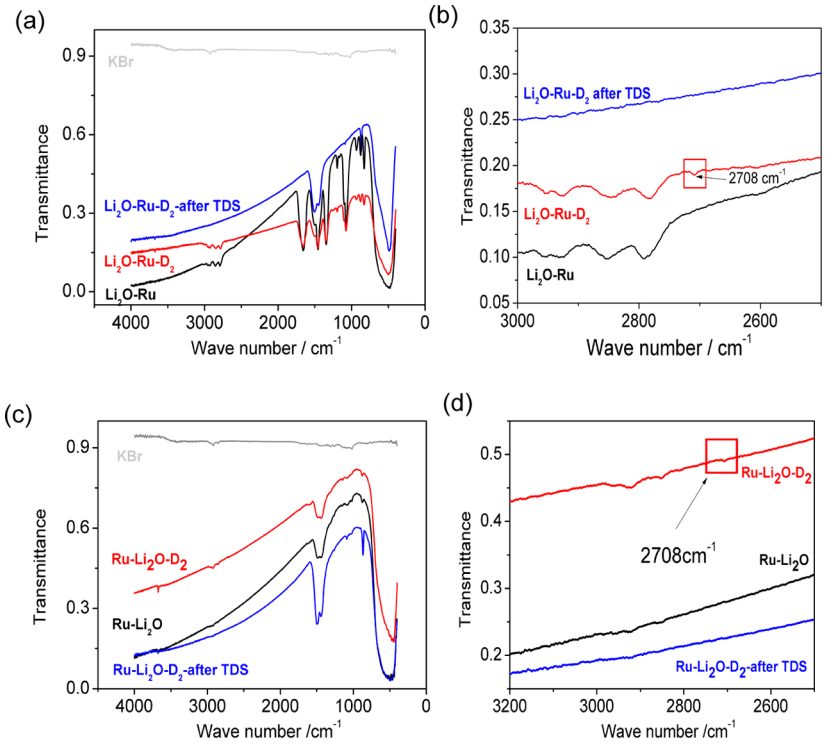

Figure 3. FTIR spectra of Ru−Li_2O prepared in different methods. (a) Full and (b) zoom-in spectra of sample ball-milled with DMC; (c) full and (d) zoom-in spectra of sample ball-milled with hexane.

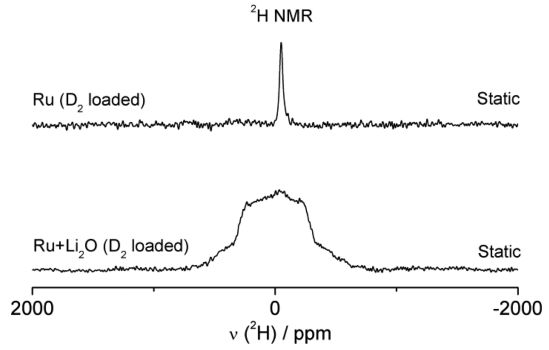

Figure 4. Solid-state static ^2H NMR spectra of D_2 loaded ruthenium nanoparticles and Ru/Li_2O.

spectrum of Ru after D_2 loading. This indicates the existence of a highly mobile deuterium species, that is, one that is fast on the NMR time scale. In contrast, for the Ru/Li_2O a comparatively broad spectral line is obtained. The outer flanks of this spectrum are consistent with a uniaxial powder pattern caused by the quadrupolar interaction with a quadrupolar coupling constant (Qcc) of about 60 kHz, whereas the Qcc of crystalline LiOD has been reported to be about 300 kHz.[33] The D atom in our composites therefore appears to be much more mobile than in crystalline LiOD, implying that the deuterium is comparatively weakly bound in the composites. The line shape of the ^2H NMR spectrum of Ru/Li_2O deviates from the theoretically predicted shape[32] with the expected trough in the center being "filled in". The most likely explanation for this is that the recorded line shape is a superposition of subspectra. These subspectra exhibit different degrees of dynamic averaging, indicating that a distribution of deuterium mobility exists, which may include chemically bound D^+ (and D^-, if D^+/D^- storage mechanism favors). In addition, previous literature reported decomposition of LiOH/LiOD to start at 400 °C, which is much higher than our results, and to produce a sustainable amount of water.[34] Hence, the ^2H NMR results are consistent with a mobile, unbound D_2 species in Ru, whereas for D_2 in the Ru−Li_2O the mobility of the deuterium is restricted, possibly by formation of a weak LiO···D bond.

In principle, a spillover effect could provide an explanation for the extra hydrogen storage in Ru/Li_2O, too. As Li_2O is hardly reducible, though, significant spillover of hydrogen in Ru/Li_2O is very unlikely to happen. Indeed, for an experiment where the dissociation step on the Ru was replaced by direct exposure of Li_2O to an atomic D beam,[35] the subsequent TDS-MS results from ball-milled Li_2O show that there is no obvious deuterium desorption during TDS procedure (Supporting Information Figure S8).

All in all, a synergistic storage mechanism is strongly corroborated, which relies on the presence of both Li_2O and Ru and with high interfacial area. From FTIR spectra and NMR results, D^+ was found weakly bound as LiO···D at the Li_2O side, the D^- or e^- is proposed to accommodate at the ruthenium side (Scheme 1), similar to the mechanism of interfacial lithium storage in M/Li_2O and M/LiF.[9,11,13]

Having demonstrated an interfacial effect of hydrogen storage in Ru/Li_2O, the amount of hydrogen stored per monolayer at 500 mbar can be estimated with certain assumptions (see Supporting Information). Taking Ru/Li_2O ball-milled with DMC (1/1 wt/wt) as an example, and using typical diameters for Ru cluster (∼100 nm, Supporting Information Figure S1) and nanoparticles (∼15 nm), an absorption of 0.3−2.3 D/Ru is assessed for the ruthenium side of the interface.

At the moment, we cannot clearly distinguish between H^+/e^- and H^+/H^- job-sharing. The storage isotherm may give us a further hint. As shown aforementioned in similarity to the

DOI: 10.1021/acs.nanolett.5b01320
Nano Lett. 2015, 15, 4170−4175

Scheme 1. Interfacial Hydrogen Storage in Li_2O/M Nanocomposites

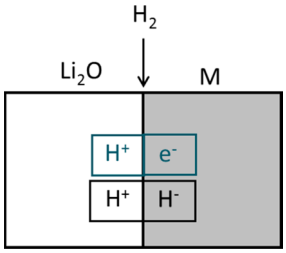

treatment of the Li-storage analogue,[9,13] we expected power laws with exponents between 1/6 and 1/8 for the first and power laws between 1/4 and 1/3 for the second case. Clearly the experimental exponents seem to follow the second mechanism (Figure 5).

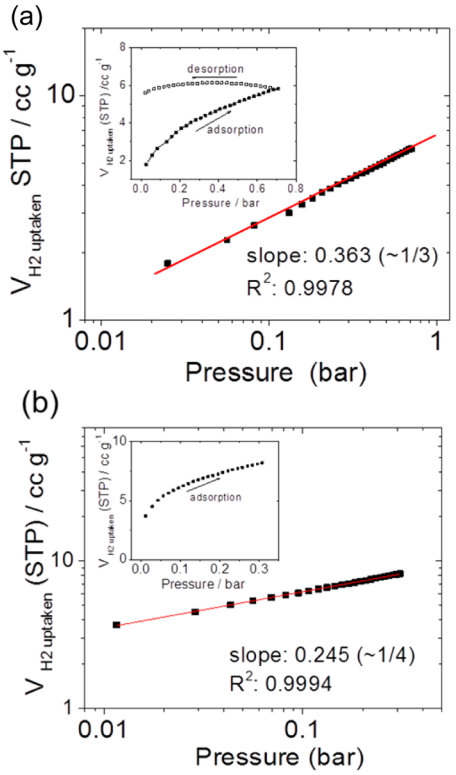

Figure 5. Hydrogen uptaken isotherm of Ru/Li_2O nanocomposites (a) freshly prepared; (b) after being stored in glovebox for 1 month. The inset of panel a shows the difficulty in reversing the hydrogenation.

There are several important points, though, to mention that weaken this argument. The first is that we do not always find power laws, however, whenever power laws are found they are very well fulfilled with exponents, that are either close to 1/3 (0.33 ± 0.03) or to 1/4 (0.25 ± 0.01) (rather than scattered around 0.3, Figure 5). A slope of 1/3 is expected for a reaction to H^+ (Li_2O) /H^- (Ru) with the negative charge solely concentrating on the first Ru-layer, while a slope of 1/4 is expected for a diffuse H^- distribution in the subsurface of Ru. A reasonable explanation could be related to the fact that the 1/4 slope that was observed for the long-term stored samples possibly exhibiting some oxygen impurities and hence made the contact layer less metallic and more semiconductive. The observation of also nonpower law situations points to kinetic complexity. The second, equally severe point refers to the difficulty in reversing the hydrogenation. This is not due to drift effects as we carefully checked by reversing the storage at various speeds and at various H-contents. We are aware of the fact that a convincing thermodynamic argumentation implies the reversibility of the data. Unfortunately the BET-apparatus does not allow us to wait for long enough to check equilibration while increasing the temperature would destroy the microstructure of the nanocomposites. Nevertheless, it may not be hopeless to construct rapidly storing composites that might be interesting for application. Irrespective of such issues, it is the fundamental mechanism of storing hydrogen by job-sharing that appears fascinating to us.

In conclusion, a novel interfacial hydrogen storage mechanism has been proposed and investigated in the Ru/Li_2O composite, in which H^+ is located at Li_2O side and H^- or e^- are located at the ruthenium side, which is similar to the lithium interfacial storage model in Li_2O/M and LiF/M. For Ru/Li_2O ball-milled in DMC (1/1 wt/wt), when loading D_2 at 500 mbar and room temperature the deuterium storage amount is 0.03 wt %. Notwithstanding the kinetic problems, the storage thermodynamics seem to favor H^+/H^- over H^+/e^-, yet this point has to be further clarified. For the example given, it is the fundamental aspect rather than technological applicability that renders it exciting.

■ ASSOCIATED CONTENT

Supporting Information

Experimental details including sample preparation, TEM, XRD, FTIR, NMR, TDS-MS, H_2 uptake/desorption measurements; methods for estimating the interface area between Li_2O and Ru phases; estimation of absorption of deuterium on Ru; TEM micrographs Ru/Li_2O nanocomposites; hydrogen isotherm sorption curves of Ru/Li_2O nanocomposites up to 20 bar at RT; detailed TDS-MS spectra of Ru/Li_2O nanocomposites; XRD patterns of Li_2O and Ru/Li_2O nanocomposites before and after D_2 uptake; solid-state MAS ^7Li NMR spectra of D_2 loaded Li_2O and Ru/Li_2O nanocomposites; TDS-MS spectra of different Li_2O samples after absorption of atomic deuterium. The Supporting Information is available free of charge on the ACS Publications website at DOI: 10.1021/acs.nanolett.5b01320.

■ AUTHOR INFORMATION

Corresponding Authors

*E-mail: l.fu@fkf.mpg.de; lijunfufu@sina.com (L.F.).
*E-mail: d.samuelis@fkf.mpg.de (D.S.).
*E-mail: s.weiglein@fkf.mpg.de (J.M.).

Author Contributions

The manuscript was written through contributions of all authors. All authors have given approval to the final version of the manuscript.

Notes

The authors declare no competing financial interest.

■ ACKNOWLEDGMENTS

We thank Ms. V. Duppel and Dr. X. Mu for TEM measurement, Dr. O. Gerbig and Mr. R. Koenig for FTIR measurement, Dr. J. Tong and Dr. Y. Chen for XRD measurement, Dr. I. Moudrakovski for NMR discussion, and

DOI: 10.1021/acs.nanolett.5b01320
Nano Lett. 2015, 15, 4170−4175

Dr. R. Merkel, Dr. L. Wang, Dr. C. Li, and Dr. Y. S. Hu for useful discussion.

REFERENCES

(1) Schlapbach, L.; Zuttel, A. *Nature* **2001**, *414*, 353−358.
(2) Hirscher, M.; Becher, M. *J. Nanosci. Nanotechnol.* **2003**, *3*, 3−17.
(3) Hirscher, M.; Becher, M.; Haluska, M.; von Zeppelin, F.; Chen, X.; Dettlaff-Weglikowska, U.; Roth, S. *J. Alloys Compd.* **2003**, *356*−*357*, 433−437.
(4) Li, J.-R.; Kuppler, R. J.; Zhou, H.-C. *Chem. Soc. Rev.* **2009**, *38*, 1477−1504.
(5) Sakintuna, B.; Lamari-Darkrim, F.; Hirscher, M. *Int. J. Hydrogen Energy* **2007**, *32*, 1121−1140.
(6) Zaluski, L.; Zaluska, A.; Ström-Olsen, J. O. *J. Alloys Compd.* **1997**, *253*−*254*, 70−79.
(7) Orimo, S.-i.; Nakamori, Y.; Eliseo, J. R.; Züttel, A.; Jensen, C. M. *Chem. Rev.* **2007**, *107*, 4111−4132.
(8) Chen, P.; Xiong, Z.; Luo, J.; Lin, J.; Tan, K. L. *Nature* **2002**, *420*, 302−304.
(9) Fu, L.; Chen, C.-C.; Samuelis, D.; Maier, J. *Phys. Rev. Lett.* **2014**, *112*, 208301.
(10) Balaya, P.; Li, H.; Kienle, L.; Maier, J. *Adv. Funct. Mater.* **2003**, *13*, 621−625.
(11) Jamnik, J.; Maier, J. *Phys. Chem. Chem. Phys.* **2003**, *5*, 5215−5220.
(12) Hu, Y.-S.; Guo, Y.-G.; Sigle, W.; Hore, S.; Balaya, P.; Maier, J. *Nat. Mater.* **2006**, *5*, 713−717.
(13) Maier, J. *Angew. Chem., Int. Ed.* **2013**, *52*, 4998−5026.
(14) Bekaert, E.; Balaya, P.; Murugavel, S.; Maier, J.; Ménétrier, M. *Chem. Mater.* **2009**, *21*, 856−861.
(15) Hu, Y.-Y.; Liu, Z.; Nam, K.-W.; Borkiewicz, O. J.; Cheng, J.; Hua, X.; Dunstan, M. T.; Yu, X.; Wiaderek, K. M.; Du, L.-S.; Chapman, K. W.; Chupas, P. J.; Yang, X.-Q.; Grey, C. P. *Nat. Mater.* **2013**, *12*, 1130−1136.
(16) Chou, M. Y.; Chelikowsky, J. R. *Phys. Rev. Lett.* **1987**, *59*, 1737−1740.
(17) Antonov, V. E.; Belash, I. T.; Malyshev, V. Y.; Ponyatovsky, E. G. *Int. J. Hydrogen Energy* **1986**, *11*, 193−197.
(18) Prins, R. *Chem. Rev.* **2012**, *112*, 2714−2738.
(19) Chadwick, A. V.; Flack, K. W.; Strange, J. H.; Harding, J. *Solid State Ionics* **1988**, *28*−*30* (Part 1), 185−188.
(20) Islam, M. M.; Bredow, T.; Minot, C. *J. Phys. Chem. B* **2006**, *110*, 9413−9420.
(21) Juarez, R.; Parker, S. F.; Concepcion, P.; Corma, A.; Garcia, H. *Chem. Sci.* **2010**, *1*, 731−738.
(22) Fang, M.; Sánchez-Delgado, R. A. *J. Catal.* **2014**, *311*, 357−368.
(23) Maier, J. *Physical Chemistry of Ionic Materials: Ions and Electrons in Solids*; Wiley: New York, 2004.
(24) von Zeppelin, F.; Haluška, M.; Hirscher, M. *Thermochim. Acta* **2003**, *404*, 251−258.
(25) Walaszek, B.; Yeping, X.; Adamczyk, A.; Breitzke, H.; Pelzer, K.; Limbach, H.-H.; Huang, J.; Li, H.; Buntkowsky, G. *Solid State Nucl. Magn. Reson.* **2009**, *35*, 164−171.
(26) Bhatia, S.; Engelke, F.; Pruski, M.; Gerstein, B. C.; King, T. S. *J. Catal.* **1994**, *147*, 455−464.
(27) Nyquist, R. A.; Kagel, R. O. *Handbook of Infrared and Raman Spectra of Inorganic Compounds and Organic Salts*; Academic Press: New York, 1971.
(28) Silverstein, R. M.; Bassler, G. C.; Morrill, T. C. *Spectrometric Identification of Organic Compounds*, 7th ed.; Wiley: New York, 2005.
(29) Tanaka, S.; Oda, T.; Oya, Y. *J. Nucl. Mater.* **2004**, *329*−*333* (Part B), 1270−1273.
(30) Lappi, S. E.; Smith, B.; Franzen, S. *Spectrochim. Acta, Part A* **2004**, *60*, 2611−2619.
(31) Malferrari, M.; Venturoli, G.; Francia, F.; Mezzetti, A. *Spectroscopy: An International Journal* **2012**, *27*, 6.
(32) Bräuniger, T.; Jansen, M. *Z. Anorg. Allg. Chem.* **2013**, *639*, 857−879.
(33) Chiba, T. *J. Chem. Phys.* **1967**, *47*, 1592−1595.
(34) Oda, T.; Oya, Y.; Tanaka, S. *Fusion Eng. Des.* **2005**, *75*−*79*, 835−839.
(35) Bischler, U.; Bertel, E. *J. Vac. Sci. Technol., A* **1993**, *11*, 458−460.

DOI: 10.1021/acs.nanolett.5b01320
Nano Lett. 2015, 15, 4170−4175